Mode decomposition method for non-classically damped structures using

acceleration responses

J.-S. Hwang¹, *S.-H. Shin², and †H. Kim²

¹Department of Architectural Engineering, Chonnam National University, Gwangju, Korea. ²Department of Architectural Engineering, Kyungpook National University, Daegu, Korea

*Presenting author: ssh10004ok@knu.ac.kr
†Corresponding author: hjk@knu.ac.kr

Abstract

For structures with non-classical damping or closely distributed modes, it is not easy to apply the traditional modal analysis method because the damping matrix is not diagonalized by the modal matrix obtained from the mass and stiffness matrices. In this paper, a new mode decomposition method for structures with non-classical damping ratio and structures with very closely distributed modes is proposed. This method defines the generalized modes in state space, and uses the differential state variables estimated from measured acceleration responses to decompose modal responses. A Kalman filtering is utilized to calculate the linear transformation matrix of governing modes, and the linear transformation matrix is updated in the optimization process to maximize the performance index cooperated with a power spectral density of a target mode. For the verification of the proposed method, a numerical simulation is performed using a single degree of freedom (SDOF) system coupled with a tuned mass damper (TMD) which represents a non-classically damped system with closely distributed modes. The results from the simulations show that the proposed method estimates the modal responses more precisely than conventional mode decomposition methods such as the independent component analysis (ICA) method and the proper orthogonal decomposition (POD) method.

Keywords: Mode decomposition, Non-classical damping, Closely distributed mode, Linear transformation matrix, Differential state variable, Averaged power spectrum

Introduction

The response of a linear multi-degree-of-freedom (MDOF) structure is often estimated using a few governing mode responses after transforming the system into single-degree-of-freedom (SDOF) systems in the modal space. The transformation into the modal space in the modal analysis requires the modal matrix that is composed of mode shapes, and thereby it is necessary to obtain the mode shapes primarily.

The mode shapes or modal matrix is generally obtained from the eigenvalue analysis using mass and stiffness matrices of the finite element analysis model. The mass and stiffness matrices of the actual structure, however, differ from those of the analysis model yielding the discrepancy in the dynamic characteristics and mode shapes. Further, it is not possible to separate modes using the mode shapes obtained from the mass and stiffness matrices if a structure has non-classical damping that is not proportional to mass and stiffness matrices or the structure has closely distributed modes.

In order to estimate the actual mode shapes for accurate modal separation, the mode decomposition method using measured structural responses has been studied. In special, the mode separation methods using the measured responses from appropriately numbered sensors have been developed because the behavior of a building structure subjected to wind load is governed by a few lower mode responses.

The proper orthogonal decomposition (POD) method is one of the mode decomposition methods using the linear transformation of measured responses [Feeny (2002); Han and Feeny (2003)]. The POD method, also called as the principal component analysis (PCA) method, Karhunen-Loeve method, or the singular value decomposition (SVD) method [Gramaand and Subramanian (2014); Khalil and Sarkar (2014)], transforms the higher order model into the lower order model with

orthogonal basis minimizing the loss of higher order model information. The independent component analysis (ICA) method is another mode decomposition method using the linear transformation of measured responses based on the assumption that modes are independent each other [Roberts and Everson (2001); Kerschen and Poncelet (2007)]. It is also possible to perform the mode decomposition using the output-only method such as the stochastic subspace identification (SSI) and frequency domain decomposition (FDD) methods, which estimates the modal characteristics of a structure using the measured responses [Van Overschee and De Moor (1996); Brincker et al. (2001); Ku et al. (2007)].

These mode decomposition methods are applicable to structures with classical damping, which is proportional to mass and stiffness matrices. Further, they yield reliable results when buildings have very small damping ratio and thereby possess the characteristics of structures with classical damping. The ICA method, which is mostly close to the method proposed in this paper, assumes that modes are separated enough to be independent each other. However, the damping matrix is not proportional to mass and stiffness matrices of actual structures and it is not appropriate to assume that the closely distributed modes are independent each other. Therefore, there exists a limit when the previous mode decomposition methods are applied to structures with non-classical damping or with closely distributed modes.

In this paper, the new mode decomposition method using only measured responses is presented for structures with non-classical damping or with closely distributed modes. This mode decomposition method applies the linear transformation to measured response for calculating the modal responses similarly to the ICA method. The linear transformation matrix differs from that of the ICA method such that it is obtained by optimizing the objective function. The objective function is given to maximize the energy at the certain mode and to minimize the difference between averaged modal response spectrum and the linear transformation matrix assuming that each mode possesses unique pole with one natural frequency and one damping ratio.

For the verification of the proposed mode decomposition method, the numerical simulation of a two DOF system with a tuned mass damper (TMD) that is a representative system with non-classical damping and very closely distributed modes. It is assumed in the numerical simulation that the external load has wide spectral range like wind loads and the only responses of the main structure and TMD are measurable. The mode shapes and modal responses obtained from the measured responses are compared to the analytical ones to verify the proposed mode decomposition method.

Mode decomposition in state-space domain

Estimation of unmeasured state variables

The mode decomposition of a structure with non-classical damping is not possible because the damping matrix cannot be diagonalized using the mass and stiffness matrix. This requires having linear combination of state-space variables to construct modal responses.

The mode shapes of an MDOF system whose governing equation is given in Eq. (1) are defined as the linear combination as in Eq. (2). The mode separation is possible only when the damping matrix, C, is diagonalized by the mode shape matrix, Φ , in Eq. (3), which is obtained from the eigenvalue analysis of mass matrix, M, and stiffness matrix, K.

$$M\ddot{x} + C\dot{x} + Kx = Ef \tag{1}$$

$$x = \Phi \eta \tag{2}$$

$$\ddot{\eta} + \Phi^T C \Phi \dot{\eta} + \Omega \eta = \Phi^T E f \tag{3}$$

where f is the external force, E is the force location matrix, Ω is the diagonal matrix with entries of squared natural frequencies, and x and η are the response vectors in time domain and modal space, respectively.

If the structure has non-classical damping, the term $\Phi^T C \Phi \dot{\eta}$ in Eq. (3) is not a diagonal matrix, and thereby the mode decomposition is not attainable. Consequently, it is required to expand the modal responses into the state-space domain for the mode decomposition. Eq. (1) is transformed into Eq.

(4) in state-space domain, and the state variable, z, can be transformed into modal space using the newly defined modal responses in state-space domain, p, as in Eqs. (5) and (6).

$$\dot{z} = Az + Bf \tag{4}$$

$$z = \Psi p \tag{5}$$

$$\dot{p} = \Psi^{-1} A \Psi \Psi + \Psi^{-1} B f \tag{6}$$

where

$$A = \begin{bmatrix} 0 & I \\ -M^{-1}K & -M^{-1}C \end{bmatrix} \tag{7}$$

$$B = \begin{bmatrix} 0 \\ -M^{-1}E \end{bmatrix} \tag{8}$$

and the mode shape in state-space domain, Ψ , satisfies

$$\hat{A} = \Psi^{-1} A \Psi = \begin{bmatrix} 0 & I \\ -\Omega & -Z \end{bmatrix} \tag{9}$$

where $Z = diag(2\xi_i\omega_i)$, diag() is the diagonalization function, and ξ_i and ω_i are the damping ratio and natural frequency of the i-th mode, respectively.

All of state variable z of displacement and velocity or differential variable \dot{z} of velocity and acceleration are necessary in order to obtain the modal responses in state-space domain of Eq. (5). However, it is not practical to measure every state and it is often to measure acceleration responses in practice. Therefore, it is assumed in this paper that the number of sensors is equal to the number of governing modes and velocity and displacement responses are obtainable from the measured acceleration using the Kalman filter.

Given that the order of Kalman filter is twice the number of sensors, the initial estimate of the system matrix A is given as

$$A_0 = S_{21} S_{dv}^{-1} (10)$$

where A_0 is the initial estimate of the system matrix A, $S_{21} = E[\dot{z} \quad z^T]$ and $S_{dv} = E[z \quad z^T]$. Multiplying Eq. (4) by z^T and averaging yields Eq. (10). The external force term is ignored since it is not known or measurable.

Since the velocity and displacement are required in Eq. (10), the following simple integrating filter is introduced.

$$\begin{pmatrix} \dot{q} \\ \ddot{q} \end{pmatrix} = \begin{bmatrix} 0 & 1 \\ 0 & 0 \end{bmatrix} \begin{pmatrix} q \\ \dot{q} \end{pmatrix} + \begin{pmatrix} 0 \\ 1 \end{pmatrix} \ddot{x}_m$$
 (11)

where \ddot{x}_m is the measured acceleration, and q and \dot{q} are displacement and velocity integrated from the measured acceleration, respectively.

If the measured acceleration in Eq. (11) is biased, the integrated displacement and velocity have considerable amount of errors and often diverge during integration. In order to avoid the divergence and to minimize the errors, the control variable, u, is added to Eq. (11) as in Eq. (12) where the control gain, G, of size 1x2 is decided to minimize the squared displacement and squared control variable in Eq. (13).

$$\begin{pmatrix} \dot{q} \\ \ddot{q} \end{pmatrix} = \begin{bmatrix} 0 & 1 \\ 0 & 0 \end{bmatrix} \begin{pmatrix} q \\ \dot{q} \end{pmatrix} + \begin{pmatrix} 0 \\ 1 \end{pmatrix} \ddot{x}_m + \begin{pmatrix} 0 \\ 1 \end{pmatrix} u$$
 (12.a)

$$u = -G \begin{pmatrix} q \\ \dot{q} \end{pmatrix} \tag{12.b}$$

$$J = \int_0^T \frac{1}{2} (Q_1 q^2 + Ru^2) dt$$
 (13)

where Q_1 and R are weights. Note that the control variable u is equal to the difference between the actual measured acceleration and the estimated one.

The control gain, G, can also be obtained by modifying weights Q_1 and R such that the difference between the actual measured acceleration and the estimated one is in a certain range. The more detailed process for control gain calculation including the Kalman filter method is omitted here since it has been widely introduced in many references [Hwang et al. (2011)].

Objective function for mode decomposition

Once the state variables are estimated from the measured acceleration responses using the Kalman filter, the relationship between the state variables and the modal responses can be defined using Eq. (5). Because the purpose is the mode decomposition using the measured responses, Eq. (5) is rewritten as

$$p = W^T z \tag{14}$$

where $W^T = \Psi^{-1}$. Since it is assume that the number of the sensors, n, is equal to the number of governing modes, the transformation matrix, W, is a square matrix of $2n \times 2n$ and its inverse matrix exists.

It can be noted that the each column of the transformation matrix W is the combination of linear transformation coefficients that separate certain modes from the measured state variables. Since the measured acceleration and its integral value, velocity, are mostly used, Eq. (14) can be rewritten using differentiated state variables as

$$\dot{p} = W^T \dot{z} \tag{15}$$

where the entries of the transformation matrix W are constant and are not affected by differentiation.

From Eq. (15), it can be noted that the number of differentiated state variable, \dot{z} , is 2n and the number of corresponding generalized modes is also 2n. The first n modes obtained from Eq. (15) have relationship with the rest of modes defined as in Eq. (6). If the effect of external force is negligible in Eq. (6), the relationship becomes velocity to acceleration. That is, the relationship between i-th mode and (i+n)-th mode is velocity to acceleration, if $i \le n$ and the effect of external force is negligible.

The *i*-th mode can be presented using the *i*-th column of W of Eq. (15) as

$$\dot{p}_i = (W_i)^T \dot{z} \tag{16}$$

In order for the *i*-th mode obtained from Eq. (16) to be decomposed into a true vibration mode with single pole that consists of natural frequency, ω_i , and damping raito, ξ_i , the modal power spectrum obtained from Eq. (16) needs to have only one peak near the natural frequency when there is no special poles in the external force. That is, the effect of other modes should not be appeared showing no peaks near other modes.

In this paper, the following necessary conditions are defined for true mode decomposition described above. These conditions also are the preconditions to define the objective function for mode decomposition. Note that these conditions are not necessary and sufficient conditions for mode decomposition and that other necessary conditions based on other idea can also be adopted.

Necessary condition 1: The total energy of decomposed modes is always constant. This condition is satisfies by setting the integral value of modal response spectrum, which is equal to the variance value, to be '1'.

Necessary condition 2: The modal energy is max near its natural frequency. The corresponding natural frequency can be obtained from the system matrix A_0 in Eq. (10).

Necessary condition 3: The effect by neighboring modes is minimized. This condition can be satisfied by minimizing the differences between the modal power spectrum and averaged power spectrum at neighboring modal frequencies.

The objective function satisfying the above necessary conditions 1 and 2 can be defined as

$$J_{12} = \int_{\omega_i - \Delta\omega}^{\omega_i + \Delta\omega} S_{ii}(\omega) d\omega + \lambda \left(\int_0^\infty S_{ii}(\omega) d\omega - 1 \right)$$
 (17)

where λ is a Lagrange multiplier for constraining the necessary condition 1, $\Delta\omega$ is the infinitesimal change of frequency, and $S_{ii}(\omega)$ is the power spectrum of the decomposed mode. $S_{ii}(\omega)$ is one-sided spectrum given as

$$S_{ii}(\omega) = W_i^T S_{va}(\omega) W_i$$
 (18.a)

$$S_{va}(\omega) = z(\omega)\bar{z}(\omega)$$
 (18.b)

where $z(\omega)$ is the Fourier transformation of differential state variable, $\dot{z}(t)$ and $\bar{z}(\omega)$ is the complex conjugate of $z(\omega)$. Substituting Eq. (18) into Eq. (17) simplifies the objective function of Eq. (17) as

$$J_{12} = W_i^T S_{peak} W_i + \lambda (W_i^T S_{var} W_i - 1)$$
 (19.a)

$$S_{peak} = \int_{\omega_i - \Delta\omega}^{\omega_i + \Delta\omega} S_{va}(\omega) d\omega$$
 (19.b)

$$S_{var} = \int_0^\infty S_{va}(\omega) d\omega \tag{19.c}$$

 S_{peak} and S_{var} are readily obtainable from the differentiated state variables directly. Consequently, the transformation matrix, W_i , for the i-th mode that satisfies the condition 1 and 2 can be derived by differentiating J_{12} of Eq. (19.a) with respect to W_i and setting the resulting value to be '0'. The result of differentiation is given as

$$(S_{peak} + \lambda S_{var})W_i = 0 (20.a)$$

$$S_{peak}W_i = -\lambda S_{var}W_i \tag{20.b}$$

It can be noted from Eq. (20) that the value of $(-\lambda)$ is the eigenvalue of two matrices, S_{peak} and S_{var} , while W_i is the corresponding eigenvector. This means that the largest eigenvalue becomes the maximum value of objective function and the corresponding eigenvector W_i becomes the linear transformation matrix.

If modes are separated enough to affect each other marginally, it is possible to perform the mode decomposition accurately using the transformation matrix obtained from Eq. (20). When modes are closely distributed, the reciprocal effect between modes becomes significant. In that case, the objective function that satisfies the necessary conditions 1 and 2 only cannot yields the accurate mode decomposition. In order to minimize the effect of neighboring modes, the following objective function that satisfies the necessary conditions 3 as well as 1 and 2 is defined.

$$J_{123} = \frac{\int_{\omega_{i}-\Delta\omega}^{\omega_{i}+\Delta\omega} S_{ii}(\omega)d\omega}{\int_{\omega_{k}-\Delta\omega}^{\omega_{k}+\Delta\omega} \left(\log\left(\frac{S_{ii}(\omega)}{S_{H}(\omega)}\right)\right)^{2}d\omega} + \lambda \left(\int_{0}^{\infty} S_{ii}(\omega)d\omega - 1\right)$$
(21)

where S_H is the averaged power spectrum given as

$$S_H(\omega) = S_o |H(s)|^2 \tag{22.a}$$

$$H(s) = \frac{s}{s^2 + 2\xi_i \omega_i + \omega_i^2}$$
 (22.b)

$$S_{o} = \frac{\int_{\omega_{i}-\Delta\omega}^{\omega_{i}+\Delta\omega} S_{ii}(\omega) d\omega}{\int_{\omega_{i}-\Delta\omega}^{\omega_{i}+\Delta\omega} |H(s)|^{2} d\omega}$$
(22.c)

where s is the Laplace variable, H(s) is the transfer function of velocity response from the external force of a SDOF system, and S_o is the constant that represents the ratio of the i-th modal power spectrum to the transfer function near the i-th mode frequency.

The difference between Eqs. (17) and (21) is that the logarithmic ratio of the *i*-th modal spectrum to the averaged spectrum near the frequency of neighboring mode, ω_k , is included in the denominator. Minimizing the ratio in the denominator maximizes the objective function, while the logarithmic ratio accentuates the difference between two spectrums. The objective function in Eq. (21) can be simplified using W_i as

$$J_{123} = \frac{W_i^T S_{peak} W_i}{\int_{\omega_i - \Delta\omega}^{\omega_k + \Delta\omega} \left(\log \left(W_i^T q_{ii}(\omega) W_i \right) \right)^2 d\omega} + \lambda \left(W_i^T S_{var} W_i - 1 \right)$$
(23)

where

$$q_{ii}(\omega) = \frac{S_{ii}(\omega)}{S_H(\omega)} \tag{24}$$

The natural frequency, ω_i , in Eq. (22.b) can be directly obtained from the system matrix of Eq. (10) while ehe damping ratio, ξ_i obtained from the system matrix has large error. Therefore, the damping ratio needs to be selected such that S_o of Eq. (22.c) satisfies the following relationship derived from the necessary condition 1.

$$\int_{0}^{\infty} S_{o}(\xi_{i}) |H(s)|^{2} d\omega - 1 = \int_{0}^{\infty} S_{ii}(\omega) d\omega - 1 = 0 \quad (25)$$

Once the values of all variables in Eq. (23) are calculated, the transformation matrix, W_i , can be obtained by differentiating the objective function with respect to W_i . However, the closed-form similar to one in Eq. (20) cannot be derived due to the nonlinearity. Therefore, the sensitivity of objective function is utilized in the optimization process to obtain the transformation matrix, W_i .

Validation of the proposed method

Example structure and its modal characteristics

A numerical simulation using an example structure with non-classical damping and very closely distributed modes is carried out to verify the proposed mode decomposition method. The example structure is a two-DOF system with a TMD which is a representative system with non-classical damping and very closely distributed modes. The dynamic characteristics of the structure and external load are summarized in Table 1. It is assumed that the low-pass filtered white noise is applied to the main structure only.

In Tables 2 and 3, the mass and stiffness matrices along with the corresponding mode shapes are presented in time and state-space domains, respectively. These mode shapes will be compared to ones obtained using the proposed mode decomposition method. It can be noted that the damping matrix is not diagonalized by the mode shape obtained from the eigenvalue analysis of mass and stiffness matrices in time domain from Table 2, while modes are apparently separated in state-space domain from Table 3.

Table 1. Dynamic characteristics of the example structure

| Description | | Value | Remark |
|---------------|------------------------------------|-----------------|--|
| Structure | Main structure mass (m_s) | 100 kg | Natural frequency of the main structure (f_0) = 0.2 Hz |
| | TMD mass (m_t) | 1 kg | Mass ratio of TMD mass to main structure mass = 0.01 |
| | Main structure stiffness (K_s) | 157.9137 N/m | |
| | TMD stiffness (K_t) | 1.5635 N/m | |
| | Main structure damping | 2.5133 N·s/m | Main structure damping ratio $(\xi_s) = 0.01$ |
| | TMD damping | 0.1250 N·s/m | TMD damping ratio (ξ_t) = 0.05 |
| External load | Filter | Low pass filter | Zero to 4 Hz |
| | Sampling time | 0.005 s. | Sampling frequency = 200 Hz |
| | Duration | 3600 s. | |

Table 2. Analytically obtained modal properties in time domain

| Matrix | Symbol | Value | |
|----------------------------|-----------------------|---|--|
| Mass matrix | M | $\begin{bmatrix} 100 & 0 \\ 0 & 1 \end{bmatrix}$ | |
| Damping matrix | C | $\begin{bmatrix} 2.6383 & -0.1250 \\ -0.1250 & 0.1250 \end{bmatrix}$ | |
| Stiffness matrix | K | [159.4772 -1.5635] -1.5635 1.5635] | |
| Natural frequencies | ω_1 ω_2 | 1 st mode: 1.1925 (0.1898 Hz) 2 nd mode: 1.3177 (0.2097 Hz) | |
| Mode shapes | Φ | $\begin{bmatrix} -0.0671 & -0.0741 \\ -0.7415 & 0.6710 \end{bmatrix}$ | |
| Transformed damping matrix | $\Phi^T C \Phi$ | $\begin{bmatrix} 0.0682 & -0.0503 \\ -0.0503 & 0.0832 \end{bmatrix}$ Damping ratio of diagonal terms = $(0.0286\ 0.0316)$ | |

It can be noted that even though the transformed damping matrix in Table 2 is not a diagonal matrix, the diagonal entries, $(0.0682\ 0.0832)$, are very close to those of damping part of mode transformed system matrix, \hat{A} , in Table 3. It can be also noticed that the natural frequencies in time domain, $0.1898\ Hz$ and $0.2097\ Hz$, and those in state-space domain, $0.1910\ Hz$ and $0.2095\ Hz$, are very close each other, while the difference between the first and second modes is only $0.02\ Hz$ indicating the very closely distributed modes.

In Table 3, the modal matrix, Ψ , in state-space domain is shown in the ascending order of natural frequencies, and its inverse matrix, i.e. the linear transformation matrix, W, is also provided. Considering that the first two rows of load participation matrix, B, are zeros, it can be noted that the first and second columns of modal responses in state-space domain are integral values of the third and fourth columns, respectively, indicating the displacement-velocity and velocity-acceleration relationships.

Table 3. Analytically obtained modal properties in state-space domain

| Matrix | Symbol | Value |
|------------------------------|------------------------|--|
| | A | |
| Gt | | 0 0 0 1 |
| System matrix | | -1.5948 0.0156 -0.0264 0.0013 |
| | | $ \left[\begin{array}{cccc} 1.5635 & -1.5635 & 0.1250 & -0.1250 \end{array} \right] $ |
| Load participation matrices | B^{T} | [0 0 0.01 0] |
| | Ψ | $\begin{bmatrix} -0.6367 & -0.6543 & -0.2392 & 0.2131 \end{bmatrix}$ |
| Model metric | | -7.4864 6.6730 -0.2046 0.1823 |
| Modal matrix | | 0.3431 -0.3670 -0.6204 -0.6721 |
| | | 0.2934 -0.3139 -7.4725 6.6578 |
| | | [-0.7306 -0.8195 0.0396 0.0380] |
| T: | W | $\begin{bmatrix} -0.0704 & 0.0707 & -0.0396 & -0.0380 \end{bmatrix}$ |
| Linear transformation matrix | | 0 0 -0.7274 -0.8164 |
| | | 0.0253 0.0243 -0.0736 0.0676 |
| | Â | |
| Mode transformed system | | 0 0 0 1 |
| matrix | | $\begin{bmatrix} -1.4340 & 0 & -0.0681 & 0 \end{bmatrix}$ |
| | | $\begin{bmatrix} 0 & -1.7217 & 0 & -0.0833 \end{bmatrix}$ |
| | ω_i and ξ_i | Natural frequency Damping ratio |
| Eigenvalues | | 1 st mode 1.20 (0.1910 Hz) 2.85e-02 2 nd mode 1.31 (0.2085 Hz) 3.17e-02 |
| - | | 2 nd mode 1.31 (0.2085 Hz) 3.17e-02 |

Characteristics of mode decomposition depending on the objective function

A numerical analysis of the coupled main structure-TMD is performed to obtain the acceleration responses. The external load presented in Table 1 is applied in the numerical analysis.

The displacement and velocity responses are obtained using the integral filter given in Eq. (12), and the initial estimate of the system matrix is calculated using Eq. (10). Table 4 presents the covariance matrices used for calculating the initial estimate of the system matrix along with the modal characteristics.

Table 4 indicates that the natural frequencies obtained from the initial estimate of the system matrix present insignificant error compared to the exact natural frequencies given in Table 2. The damping ratios are, however, negative values indicating significant error. The modal matrix and linear transformation matrices also differ from the exact ones while the correlationship of sign between matrices is very large.

The linear transformation matrices obtained using the proposed mode decomposition method are compared to the exact one in Table 5. First, the first mode linear transformation matrix that maximizes the objective function J_{12} in Eq. (19) is obtained using Eq. (20). The vector with norm value of '1' is also presented in Table 5 for easier comparison. It can be seen that the linear transformation matrix obtained from the initial estimate of the system matrix is closer to the exact one than one obtained using the objective function J_{12} . The values in the first three rows show very close results to exact ones while the value of the last row is about 2.5 times to that of exact one.

Table 4. Covariance matrices and modal characteristics of initial estimate of system matrix

| Matrix | Symbol | Value |
|------------------------------------|------------------------|--|
| | S_{dv} | 17.51 21.86 0.01 105.39 |
| Covariance matrix of state | | 21.86 866.02 -105.30 0.18 |
| variable | | 0.01 -105.30 27.15 20.09 |
| | | [105.39 0.18 20.09 1333.47] |
| | S_{21} | 0.01 -105.30 27.15 20.09 |
| Chara carration as matrix | | 105.39 0.18 20.09 1333.47 |
| Cross covariance matrix | | -27.17 -20.17 0.01 -165.63 |
| | | _19.98 |
| | | |
| Luitial actionate of avetam matrix | A_o | 0 0 0 1 |
| Initial estimate of system matrix | | $\begin{bmatrix} -1.5883 & 0.0321 & 0.1260 & -0.0006 \end{bmatrix}$ |
| | | |
| | Ψ | $\begin{bmatrix} -0.8265 & -0.7677 & -0.6655 & 0.5842 \end{bmatrix}$ |
| Modal matrix | | -8.2899 7.2777 -0.6621 0.5812 |
| wiodai matrix | | $\begin{bmatrix} 0.9368 & -1.0098 & -0.8268 & -0.7675 \end{bmatrix}$ |
| | | 0.9320 -1.0046 -8.2903 7.2780 |
| | W | [-0.5944 -0.6757 0.0815 0.0757] |
| Linear transformation matrix | | $\begin{bmatrix} -0.0555 & 0.0728 & -0.0815 & -0.0757 \end{bmatrix}$ |
| Linear transformation matrix | | 0 0 -0.5879 -0.6697 |
| | | 0.0521 0.0484 -0.0620 0.0668 |
| | ω_i and ξ_i | Natural frequency Damping ratio |
| Eigenvalues | | 1 st mode 1.19 (0.1894 Hz) -2.08e-04 2 nd mode 1.31 (0.2085 Hz) -1.74e-04 |

Table 5. Comparison of the first mode linear transformation matrix: values in parenthesis are normalized vectors

| MOTHER TOUCH | | | | |
|--|---------|--|--|--|
| Method | Symbol | Value | | |
| Exact solution | W_1^T | $\begin{bmatrix} -0.1705 & -0.0164 & 0 & 0.0059 \end{bmatrix}$ $\begin{bmatrix} -0.9948 & -0.0959 & 0 & 0.0345 \end{bmatrix}$ | | |
| Initial estimate of system matrix | W_1^T | $ \begin{bmatrix} -0.1844 & -0.0172 & 0 & 0.0162 \\ (-0.9919 & -0.0926 & 0 & 0.0870) \end{bmatrix} $ | | |
| Objective function J_{12} in Eq. (19) | W_1^T | $\begin{bmatrix} -0.1405 & -0.0212 & 0.0001 & 0.0130 \end{bmatrix} $ $\begin{pmatrix} -0.9847 & -0.1485 & 0.0006 & 0.0914 \end{pmatrix}$ | | |
| Objective function J_{123} in Eq. (23) | W_1^T | $\begin{bmatrix} -0.1735 & -0.0157 & -0.0001 & 0.0055 \end{bmatrix} $ $\begin{pmatrix} -0.9945 & -0.0900 & -0.0005 & 0.0316 \end{pmatrix}$ | | |
| ICA | W_1^T | $\begin{bmatrix} -0.0295 & -0.0094 & -0.0337 & 0.0010 \end{bmatrix} $ $\begin{pmatrix} -0.6442 & -0.2054 & -0.7365 & 0.0212 \end{pmatrix}$ | | |

The first mode linear transformation matrix that maximizes the objective function J_{123} in Eq. (23) is also presented in Table 5. It can be seen that the values of the first three rows are almost identical to exact ones while the value of the last row has error of about 20%.

The optimization process for maximizing the objective function J_{123} is presented in Fig. 1. The initial values used in the optimization iteration are the values that maximize the objective function J_{12} . It can be seen from Fig.1 that the value of the objective function increases gradually as the iteration number increases, and it converges to a certain value as the iteration number is about 200. Among the various optimization methods, the simple gradient method is used in this paper. The linear transformation matrix is updated at the *i*-th iteration as

$$W_{i+1} = W_i + 0.001 \delta W \tag{26}$$

where

$$\delta W = \frac{\partial J_{123}}{\partial W_1} \tag{27}$$

Figure 1 also presents the iteration results of the denominator and numerator of Eq. (23) along with the error between the estimated first mode linear transformation matrix and exact one. The error is calculated as

$$\varepsilon = \sum_{j=1}^{4} \left(\left| \frac{\left(W_1 \right)_j}{\left\| W_1 \right\|} \right| - \left| \frac{\left(W_{exact} \right)_j}{\left\| W_{exact} \right\|} \right| \right)$$
 (28)

where W_{exact} is the exact first mode linear transformation matrix presented in Table 5. It can be seen that the error approaches to zero as the iteration numbers increases.

Figure 2 shows the damping ratio estimation process for the averaged power spectrum of Eq. (22) used in the optimization of the objective function J_{123} . It can be noticed that the area of the power spectral function becomes almost same to that of the averaged spectrum near the damping ratio of 0.026. Using this damping ratio and the first mode frequency, the objective function J_{123} is optimized.

The first modal spectrums obtained from the different mode decomposition method are compared to the exact one in Figure 3. It can be seen that the modal spectrums decomposed using the initial estimate of the system matrix and the objective function J_{12} are distorted considerably near the second mode frequency. In special, the decomposed modal spectrum obtained using the objective function J_{12} is continuously smaller above the second mode frequency. On the contrary, the decomposed modal spectrum obtained using the objective function J_{123} matches the exact one closely.

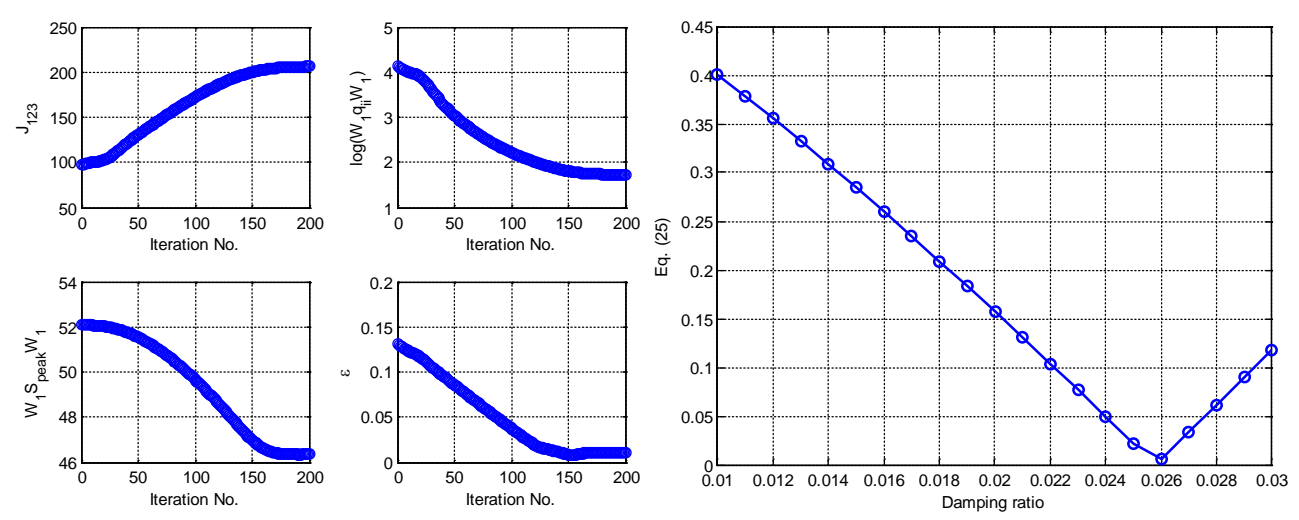


Figure 1. Iteration result

Figure 2. Damping ratio estimation

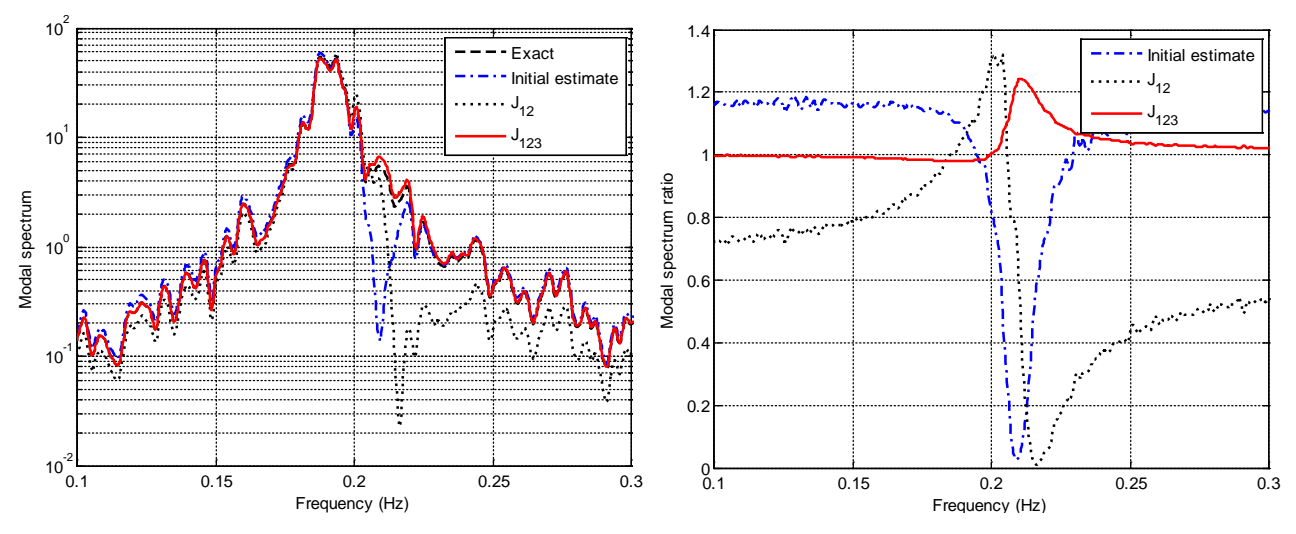


Figure 3. Modal spectrum comparison

Figure 4. Modal spectrum ratio to exact one

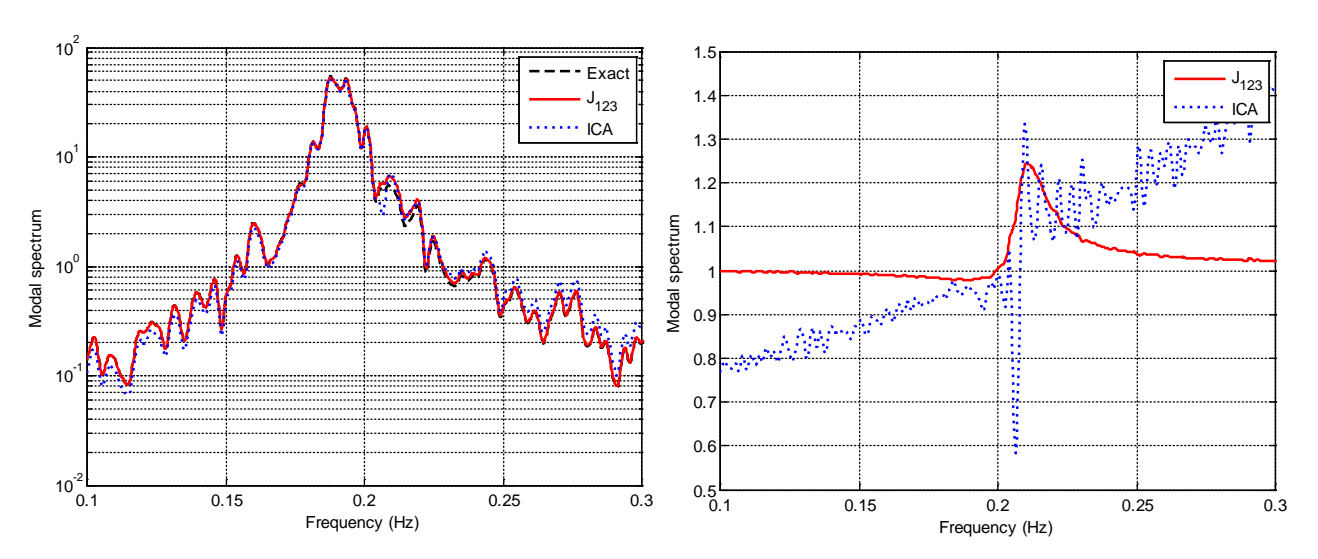


Figure 5. Modal spectrum comparison

Figure 6. Modal spectrum ratio to exact one

In order to compare the decomposed modal spectrum more closely, the ratios of decomposed modal spectrums to exact one are presented in Figure 4. It can be noticed the more distinguished error in the decomposed modal spectrum obtained using the initial estimate of the system matrix and the objective function J_{12} . The decomposed modal spectrum obtained using the objective function J_{123} shows the ratio near one meaning almost identical result except near the second mode frequency. Therefore, it can be concluded that the objective function defined in this paper yields the decomposed mode with minimum effect from the neighboring modes even when the structure has very closely distributed modes.

For the comparison of the proposed method to the previous mode decomposition methods, the decomposed first modal spectrum using the ICA method is compared in Figure 5. The modal spectrum ratios to exact one are also compared in Figure 6. The corresponding linear transformation matrix for the first mode is presented in Table 5.

It can be noticed that the modal spectrum ratio obtained using the ICA method is close to unity only near the first mode frequency. However, the ratio abruptly decreases near the second mode frequency and increases continuously above that frequency. This is because the ICA method matches the spectral area in average sense trying to maximize the modal independency from the neighboring modes. This feature of the ICA method leads the decrease or increase of the ratio where the modal frequencies do not exist. The other decomposition methods such as the POD and

PCA methods are also examined, but their results are provided here because their decomposition resolutions are far less than the ICA method.

In addition to the first mode decomposition, the second to fourth mode decompositions are also performed and their results are compared to exact ones. The results show that the mode decomposition using the objective function J_{123} also yields very close modal spectrums to exact ones for higher modes. Since the results are almost identical to that of the first mode, they are not presented here.

Conclusions

The new mode decomposition method is proposed and validated numerically. The proposed method can improve the decomposition resolution for structures with non-classical damping and closely distributed modes whose mode decomposition is difficult due to non-diagonalization of damping matrix and strong correlation between neighboring modes.

The proposed method defines a generalized mode in state-space domain and performed the mode decomposition using the state variable estimated from the measured responses. The numerical simulation using a SDOF-TMD system indicates that the objective function using the averaged spectrum with single pole yields the best mode decomposition results. Further, it is shown that the proposed method yields the decomposed mode with minimum effect from the neighboring modes even when the structure has very closely distributed modes compared to results to those of the ICA and POD methods.

References

- Li, Y., Liu, G. R., Luan, M. T., Dai, K. Y., Zhong, Z. H., Li, G. Y. and Han, X. (2007) Contact analysis for solids based on linearly conforming radial point interpolation method, *Computational Mechanics* **39**, 537–554.
- Grama, S. N. and Subramanian, S. J. (2014) Computation of Full-field Strains Using Principal Component Analysis, *Experimental Mechanics* **54**(6), 913-933.
- Khalil, M. and Sarkar, A. (2014) Independent Component Analysis to enhance performances of Karhunen–Loeve expansions for non-Gaussian stochastic processes: Application to uncertain systems, *Journal of Sound and Vibration* **333**(21), 5600–5613.
- Hwang, J.-S., Kareem, A., and Kim, H. (2011) Wind load identification using wind tunnel test data by inverse analysis, *Journal of Wind Engineering and Industrial Aerodynamics* (99), 18-26.
- Feeny, B. (2002) On Proper Orthogonal Coordinates as Indicators of Modal Activity, *Journal of Sound and Vibration* (255), 805-817.
- Han, S. and Feeny, B. (2003) Application of Proper Orthogonal Decomposition to Structural Vibration Analysis, *Mechanical System and Signal Processing* (17), 989-1001.
- Roberts S. and Everson.R. (2001) Independent Component Analysis: Principles and Practice, Cambridge Univ.
- Kerschen G, Poncelet F., and Golinval J.-C. (2007) Physical interpretation of independent component analysis in structural dynamics, *Mechanical Systems and Signal Processing* (21), 1561-1575.
- Van Overschee, P. and De Moor, B. (1996) Subspace identification for Linear Systems, Kluwer Academic Publishers.
- Brincker, R., Zhang, L., and Andersen, P. (2001) Modal identification of output-only systems using frequency domain decomposition, *Smart Materials and Structures* (10), 441-445.
- Ku, C.J., Čermark, J.E., and Chou, L.S. (2007) Random decrement based method for modal parameter identification of a dynamic system using acceleration responses, *Journal of Wind Engineering and Industrial Aerodynamics* (95), 389-410.